Photodissociation of *o*-Nitrotoluene between 220 and 250 nm in a Uniform Electric Field†

Karen J. Castle, James E. Abbott, Xianzhao Peng, and Wei Kong*

Department of Chemistry, Oregon State University, Corvallis, Oregon 97331-4003

Received: March 9, 2000; In Final Form: July 12, 2000

Measurements of the NO product from photodissociation of *o*-nitrotoluene between 220 and 250 nm were performed using one laser for dissociation and detection. The NO fragment was observed in $v'' = 0-2$ vibrational states with an average vibrational energy of 1760 cm^{-1}. The rotational distributions were non-Boltzmann, with average rotational energies of 2050, 1900, and 460 cm^{-1} for the $v'' = 0$, 1, and 2 vibrational levels. Although the quantitative results should be treated with caution due to the variation in the dissociation energy inherent to this type of one laser experiment, this work reveals some significant similarities and differences between nitrotoluene and other nitro compounds, such as nitrobenzene. The direction of the transition dipole moment was determined by orienting gas phase molecules with a strong, uniform electric field prior to dissociation with linearly polarized light. For all of the rotational transitions studied, a 46% enhancement in the NO signal was observed when the photolysis beam was polarized perpendicular rather than parallel to the orientation field. This indicated a predominantly perpendicular relationship between the transition dipole and the permanent dipole of the molecule. The degree of enhancement was less than that predicted of a pure perpendicular transition; thus we propose that a second potential energy surface was simultaneously accessed through a parallel transition. This transition was found to contribute about 15% to the overall oscillator strength.

1. Introduction

Interest in the dissociation dynamics of organic nitro compounds originates from the explosive nature of these compounds. The dissociation of small nitroalkyl[1−8] and nitroaromatic[9−23] compounds has been studied extensively. Upon UV absorption, these compounds typically produce NO_2 and NO fragments. Several groups have agreed that the major channel in dissociation of nitromethane at 193 nm is the production of CH_3 and NO_2 fragments.[1,6,7] Secondary dissociation of the NO_2 is responsible for most of the observed NO ($X^2\Pi$) and O (^3P) fragments.[7] Another mechanism leading to the NO product, suggested by Wodtke et al., involves the isomerization of nitromethane to methyl nitrite prior to dissociation.[3] A minor channel resulting in electronically excited NO ($A^2\Sigma^+$) fragments has also been reported.[7] The dissociation of nitrobenzene between 226 and 280 nm is similar to that of nitromethane at 193 nm. In the case of nitrobenzene, there are two primary channels, which lead to the production of either NO_2 or O fragments, and two minor channels, which both produce NO.[18] The two possible dissociation mechanisms yielding NO fragments are (1) a two-step mechanism first producing nitrogen dioxide and subsequently NO and (2) rearrangement of nitrobenzene to a phenyl nitrite intermediate before dissociation to NO and C_6H_5O.[18] A theoretical study by Glenewinkel-Meyer and Crim[19] has shown that the phenyl nitrite intermediate is a metastable state that leads to production of NO and phenoxy radicals. Although the phenyl nitrite intermediate has not been consistently observed, Marshall et al.[17] found that the distribution of NO fragments from dissociation of nitrobenzene is different from that of NO fragments from nitrogen dioxide. This observation undermines the probability of the sequential dissociation pathway.

Dissociation of the nitrotoluene isomers has not been studied extensively. In a femtosecond mass spectroscopic experiment at 375 nm, NO_2 and NO loss channels have been observed for all three nitrotoluene isomers.[20] The *p*-nitrotoluene isomer has also exhibited a small peak corresponding to the loss of O fragments. In the dissociation of *o*-nitrotoluene, OH is a significant product that can be attributed to the so-called "ortho effect".[14,16,20] The proximity of the methyl and nitro groups leads to steric interactions. Consequently, the ground-state geometry of *o*-nitrotoluene is unlike that of its isomers, characterized by a twisting of the NO_2 group from the plane of the aromatic ring.[22] A dissociation mechanism involving bicyclic intermediates, and possibly, rearrangement to the nitrite form prior to fragmentation has been suggested to explain the OH channel.[16] The hydrogen atom in the OH product has been shown to come exclusively from the methyl group.[16] The NO fragment from dissociation of *o*-nitrotoluene between 224 and 238 nm has also been observed by Marshall et al.[17] In this study, it was noted that the product internal energy distributions were unlike those of NO fragments from dissociation of nitrobenzene or NO_2. Whether this conclusion is supportive of the isomerization pathway is still unclear. To our knowledge, there has been no theoretical study of the molecular rearrangement pathway for the nitrotoluene isomers, analogous to the work on nitrobenzene by Glenewinkel-Meyer and Crim.[19]

Measurements of symmetry properties of the excited electronic states of nitroaromatic compounds have proven challenging. Experimental difficulties arise from the broad, featureless absorption spectra and slow dissociation of these compounds, resulting in an isotropic distribution of photofragments and low translational energy release.[18] These properties are typical of large molecules and often hinder investigations using conventional gas phase techniques such as Doppler or other photofragment translational spectroscopic methods. Furthermore, theoretical studies on nitrobenzene, the simplest of the nitroaro-

† Part of the special issue "C. Bradley Moore Festschrift".

* Corresponding author. E-mail: Kongw@chem.orst.edu. Fax: 541-737-2062.

10.1021/jp0009150 CCC: $19.00
Published on Web 08/19/2000

matic compounds, have produced contradictory results.[9−11,15,19,21] The need for a better experimental technique for studies of these complex systems is impending.

A straightforward approach for deriving vectorial information on large, complex systems is polarization spectroscopy through steric control of reactants. If parent molecules are effectively oriented, the dependence of the yield of photofragments on the polarization direction of excitation leads to direct measurement of the direction of the transition dipole moment. Among the many approaches for steric control, such as hexapole fields,[24−26] collision-induced processes,[27,28] laser-related techniques,[29,30] and uniform electric fields,[31−36] the latter is advantageous due to its simplicity. Known as the "brute force" method, this approach is achieved through electrostatic interactions between a strong, uniform electric field and the permanent dipole moment of a polar species.[37−39] When this interaction is strong enough, a preferred orientation of the molecule is induced, and the permanent dipole becomes predominantly parallel to the electric field. Orientation by this method has been routinely achieved for samples with permanent dipoles larger than 2 D and rotational temperatures less than 3 K.[40−46]

We have demonstrated the effectiveness of this field-induced orientation technique for determination of directions of transition dipoles in several studies.[40−46] Measurements of the linear dichroism of the $\pi^* \leftarrow$ n transitions of pyrimidine and pyridazine following orientation of the permanent dipole moment indicated perpendicular relationships between the permanent dipole and the transition dipole.[41,42] The dissociation dynamics of ICN and BrCN were studied by measuring CN fragments following dissociation of oriented parent molecules.[40,43,44] A quantitative approach for determining the direction of the transition dipole moment from this type of measurement was developed. While the dissociative transition of ICN at 266 nm was found to resemble a pure parallel transition, dissociation of BrCN at 213 nm had one-third contribution from a perpendicular transition.[43] The first two excited singlet states of *tert*-butyl nitrite were studied from measurements of the NO fragment.[45] The $S_1 \leftarrow S_0$ transition was found to be perpendicular while the $S_2 \leftarrow S_0$ transition was parallel to the permanent dipole of the molecule. Most recently, the direction of the dissociative transition dipole of nitrobenzene between 230 and 250 nm was reported.[46] The relationship between the permanent dipole and the transition dipole was found to be predominantly perpendicular, with 20% parallel character.

In the current work, measurements of the NO fragment from dissociation of *o*-nitrotoluene between 220 and 250 nm were performed, and internal energy distributions were characterized. Directions of transition dipole moments at these dissociation wavelengths were determined from measurements of the polarization spectroscopy of oriented parent molecules. The results were compared with studies of related organic nitro compounds.[1−23,46] These observations provided an understanding of the photodissociation dynamics and relevant potential energy surfaces of *o*-nitrotoluene.

2. Experimental Section

A detailed description of the experimental apparatus was given in a previous publication.[41] Briefly, a differentially pumped molecular beam machine was used to produce a supersonically cooled and collimated molecular beam. Room-temperature *o*-nitrotoluene (Aldrich, 99+%) vapor was seeded in helium prior to expansion through a pulsed nozzle. A stagnation pressure of 1300 Torr was used throughout the experiment to simultaneously keep a low rotational temperature and to prevent cluster formation. Variation of the stagnation pressure below 1400 Torr resulted in no significant change in the rotational distribution of the NO fragments, supportive of a negligible cluster concentration. The rotational temperature of the molecular beam was measured by replacing the *o*-nitrotoluene sample with pyrimidine (1,3-diazine).[42] From the rotationally resolved REMPI spectrum of the $\pi^* \leftarrow$ n transition in pyrimidine, the rotational temperature was found to be 2.5 K, although in some incidences, a slightly lower temperature was implied. The orientation field was generated using two parallel electrodes connected to voltage supplies of opposite polarity, and field strengths up to 50 kV/cm were used.

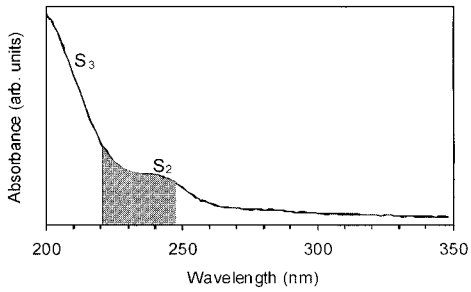

Figure 1. Gas phase absorption spectrum of *o*-nitrotoluene. The shaded region indicates the wavelength range studied in this experiment.

A Nd:YAG (Spectra Physics, GCR 230) pumped dye laser (LAS, LDL 2051) system was frequency doubled for dissociation of *o*-nitrotoluene between 220 and 250 nm. The same laser was also used to probe the NO fragments using (1 + 1) resonantly enhanced multiphoton ionization (REMPI) through the A $^2\Sigma^+$ state. Ions were detected with a time-of-flight spectrometer located beneath the electrodes. A mesh-covered hole in the bottom electrode allowed ion transmission, and the orientation field also served as the ion extraction field. The polarization direction of the laser was rotated with a half-wave plate (CVI, QWPO-226-10-2). To probe the relative yield of NO under different polarization directions of the excitation laser in high fields, the laser power was kept between 0.5 and 1.0 mJ, and the beam was focused to a diameter of approximately 1 mm. Saturation of the NO transition eliminated the effect of fragment alignment due to dissociation, so the variation in the yield of NO was solely an effect of the polarization direction of the dissociation laser. To derive the population distribution of NO, however, precautions were taken to avoid possible saturation, and the dependence of the line shape and intensity of the ion signal on the laser power was monitored. The laser power was kept below 0.3 mJ and the beam size was expanded to 2−3 mm in diameter. Two Pellin-Broca prisms, arranged as mirror images of each other, were used to separate the second harmonic from the fundamental beam emerging from the dye laser. The beam path remained very stable for scans of a few nanometers. A complete spectrum was obtained by connecting several discrete segments and correcting for shifts in the beam path. It is worth noting that in this one laser experiment, as the probe laser scanned through the resonances of NO, the dissociation energy was also changed. The population distribution thus derived should only be representative of the system when the dissociation dynamics is independent of the dissociation energy.

3. Results and Discussion

A. Photodissociation under Field-Free Conditions. The gas phase absorption spectrum of *o*-nitrotoluene between 200 and 350 nm is given in Figure 1. The shaded region indicates the

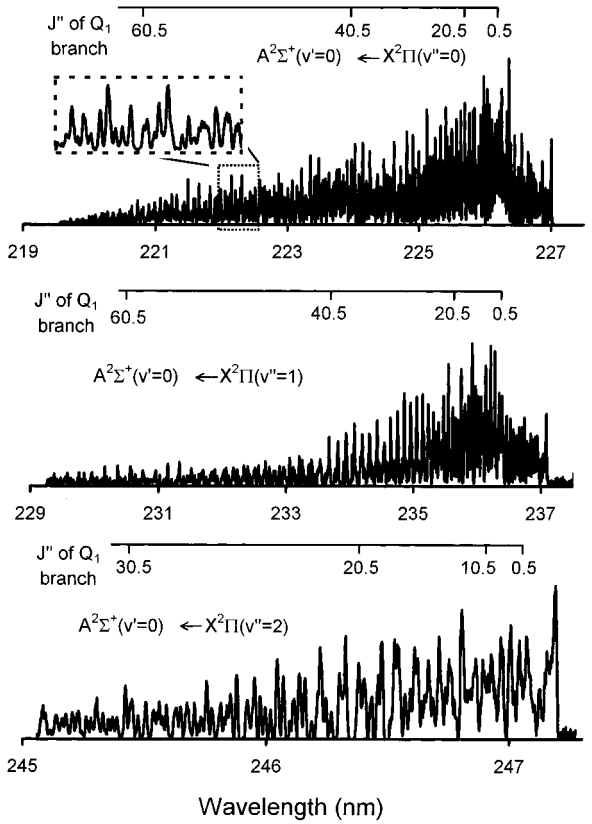

Figure 2. REMPI spectra of three vibrational bands of the NO fragment from photodissociation of *o*-nitrotoluene between 220 and 250 nm. Rotational transitions of the Q_1 branch are identified. The range of the abscissa for the $v'' = 2$ band is smaller than that of the $v'' = 0$ and 1 bands.

wavelengths studied in the present work. This absorption curve is very similar to that of nitrobenzene, with a small feature centered at 240 nm and a tail at longer wavelengths.[46] Calculations by Gonzalez-Lafont et al.[15] have indicated that with the exception of the S_1 state, higher excited singlet states of nitrobenzene are predominantly accessed through $\pi^* \leftarrow \pi$ type transitions. Our previous studies of nitrobenzene between 230 and 250 nm agreed with this conclusion. Similarly, the strong absorption feature of nitromethane at 198 nm was assigned as a $\pi^* \leftarrow \pi$ transition localized on the NO_2 moiety,[7] and this assignment was supported by the experiments of Butler et al. at 193 nm.[1]

Figure 2 shows the (1 + 1) REMPI spectra of three vibrational bands of the NO fragment following dissociation of *o*-nitrotoluene. Since a single laser was used for dissociation of parent molecules and detection of products, the actual dissociation wavelength varied between 220 and 250 nm. We expect that the dissociation dynamics of *o*-nitrotoluene should vary slowly with the dissociation energy, so some qualitative information should be obtainable from this one laser experiment. This assumption is further supported by the results from the polarization experiment (section B), where no observable changes in the direction of the transition dipole moment were detected for $\lambda \geq 223$ nm. Although different dynamics may exist in nitrotoluene and nitrobenzene, it is interesting to notice that in nitrobenzene, the dissociation dynamics were proven to be weakly dependent on the dissociation energy near the first absorption band.[46] Previously, we performed two-laser experiments on nitrobenzene in which the dissociation wavelength was fixed at 230, 240, or 250 nm. Our results were almost identical when a single laser was used for dissociation and

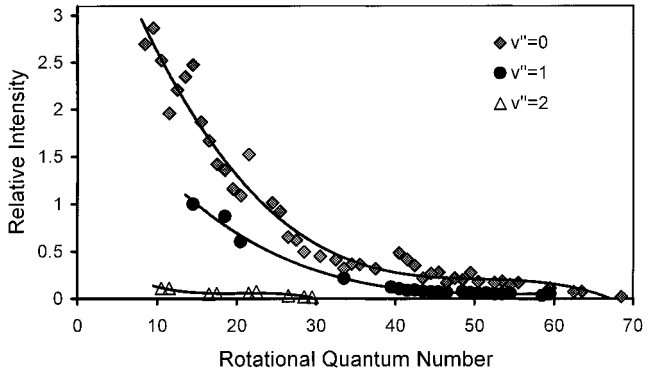

Figure 3. Vibrational and rotational populations of the NO fragment. Hönl−London factors, Franck−Condon factors, and laser power were factored into the calculations of the relative population.

detection. Furthermore, Crim's group studied the NO fragment from nitrobenzene in a single laser experiment between 220 and 227 nm.[18] The observed NO internal energy distributions were very similar to the results of our two-laser experiments.[46]

The electronic transition of NO used for detection in this experiment is a $^2\Sigma^+ \leftarrow {}^2\Pi$ transition. Spin-doublet and Λ-doublet splittings lead to 12 possible branches: Q_1 (or Q_{11}), P_1, R_1, Q_2 (or Q_{22}), P_2, R_2, Q_{12}, P_{12}, R_{12}, Q_{21}, P_{21}, and R_{21}.[47] If the spin splitting of the $^2\Sigma$ state is small, the Q_{12}, R_{12}, P_{21} and Q_{21} branches become redundant. Closely spaced rotational transitions result in spectral congestion, especially near the bandheads of several branches. Rotational levels were assigned based on the spectral simulation program LIFBASE,[48] and the Q_1 branch has been identified in Figure 2. The $v'' = 1$ spectrum has a better signal-to-noise ratio than the $v'' = 0$ band due to a greater NO signal intensity. This is attributed to the larger Franck−Condon factor of the $^2\Sigma^+$ ($v' = 0$) $\leftarrow {}^2\Pi$ ($v'' = 1$) transition and the availability of a higher laser power for this wavelength region.

The vibrational and rotational population distributions for the Q_1 branch are outlined in Figure 3. For visual guidance, trendlines are overlaid on the experimental data. The relative intensity was calculated by dividing the experimental intensity by the Hönl-London factor,[47] the Franck−Condon factor,[49] and the laser power. Since alignment parameters are not obtained in this experiment, populations in low J levels cannot be calculated with credibility and are not included in the figure. Furthermore, rotational transitions with quantum number less than 10.5 are generally not resolvable with the current laser system. The NO fragments are formed in $v'' = 0$, 1, and 2 vibrational states with relative populations of 1:0.6:0.06. The average vibrational energy is 1760 cm^{-1}, or approximately 4.6% of the available energy. All of the rotational distributions are non-Boltzmann, and fragments in the first two vibrational levels are highly rotationally excited. The average rotational energies are approximately 2050 cm^{-1} for the lowest vibrational level and 1900 cm^{-1} for the first excited vibrational level. The $v'' = 2$ level is considerably colder with an average rotational energy of 460 cm^{-1}. However, the dissociation energy at the $v'' = 2$ level corresponds to the low-energy edge of the S_2 state. The low rotational energy of this vibrational band could also be related to the low available energy. Two independent lasers are necessary to determine the origin of this variation in rotational energy distribution among different vibrational levels.

Table 1 lists the average rotational (E_r) and vibrational (E_v) energies of the NO fragment from *o*-nitrotoluene as determined in this experiment. The rotational energy for each vibrational level is listed individually, and the average rotational energy

TABLE 1: Average Rotational (E_r) and Vibrational (E_v) Energies for the NO Fragments from *o*-Nitrotoluene (*o*-NT) and Nitrobenzene (NB)[a]

	o-NT 226 nm	NB 226 nm[18]	impulsive model (NB)[18]	statistical model (NB)[18]
E_r (cm^{-1}), $v'' = 0$	2050 ± 110	2580 ± 242	9680	1610
% of E_{av}	5.4 ± 0.3	6.8 ± 0.6	25.5	4.3
E_r (cm^{-1}), $v'' = 1$	1900 ± 100			
% of E_{av}	5.2 ± 0.3			
E_r (cm^{-1}), $v'' = 2$	460 ± 25			
% of E_{av}	1.3 ± 0.1			
E_r (cm^{-1}), avg	1940 ± 110	2580 ± 242		
% of E_{av}	5.3 ± 0.3	6.8 ± 0.6		
E_v (cm^{-1})	1760 ± 90	< 810	1130	810
% of E_{av}	4.6 ± 0.2	< 2.1	3.0	2.1

[a] The available energies (E_{av}) are approximately 37 900, 36 300, and 34 700 cm^{-1} for $v'' = 0$, 1, and 2, respectively. The calculated energies for the impulsive and statistical models of energy release for nitrobenzene are also given.[18]

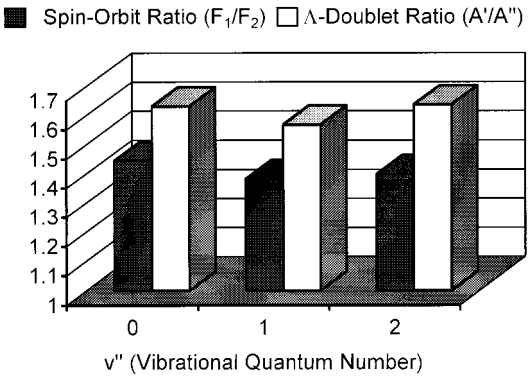

Figure 4. Populations of NO in the spin−orbit and Λ-doublet states for $v'' = 0$, 1, and 2. The average F_1/F_2 ratio is approximately 1.4, while the A′/A″ ratio is 1.7.

was obtained by taking into account the relative populations of the contributing vibrational states. On the basis of an estimated energy of the $C-NO_2$ bond of *o*-nitrotoluene, the available energy for the system is between 34 700 and 37 900 cm^{-1}, depending on photolysis wavelength.[18] Experimental and calculated energies for nitrobenzene, as obtained by Galloway et al., are also given in Table 1.[18] For nitrobenzene, the impulsive model of energy release predicts that a large fraction of the available energy will be found in rotation of the NO fragment, which does not agree with experimental observations.[18] The statistical model provides a better approximation to experiments on nitrobenzene but still fails to describe the photodissociation completely. Comparison between the present experiment on *o*-nitrotoluene and the work of Galloway et al. on nitrobenzene indicates that the NO fragment from *o*-nitrotoluene is formed with less rotational energy, but nearly twice as much vibrational energy as that from nitrobenzene. Statistical calculations on *o*-nitrotoluene cannot be performed due to a lack of information regarding the rovibronic density of states and vibrational frequencies. Moreover, the present results might be affected by variations in the excitation energy in this one laser experiment, so quantitative comparisons between our observations and theory are not performed.

Figure 4 shows the preference of the NO fragment for spin−orbit doublet and Λ doublet states. For all three vibrational bands, the NO product was preferentially produced in the low spin−orbit component (F_1) with an F_1/F_2 ratio of approximately 1.4. A preferential population of the P and R branches relative to Q branches was also observed. The Λ doublet ratio, A′/A″, for each of the three vibrational bands was approximately 1.7. Thus, the unpaired π orbital of the NO fragment lies in the plane of rotation, and A′ symmetry of the excited electronic state of *o*-nitrotoluene is implied.

To our knowledge, a complete study of the dissociation dynamics of *o*-nitrotoluene between 220 and 250 nm has not been pursued, so a comparison with studies of nitrobenzene and nitromethane will be informative. In the present experiment, a significant fraction of NO fragments from *o*-nitrotoluene was formed in the first excited vibrational state. Galloway et al.[18] placed an upper limit of 10% on the fraction of NO fragments from dissociation of nitrobenzene that could be produced in any vibrationally excited state. However, Daugey et al. reported that 30% of NO fragments from nitrobenzene were formed in vibrationally excited states.[23] For nitromethane, Moss et al.[7] found that at least 90% of the NO fragments from nitromethane were formed in the ground vibrational state. Thus, our observations, though qualitative, indicate that the NO fragment from *o*-nitrotoluene is produced with a significantly higher vibrational energy than that from nitrobenzene or nitromethane. This difference could be related to a more dramatic change in geometry during dissociation of *o*-nitrotoluene, which might be a manifestation of the perturbation caused by the nearby methyl group. It is interesting to notice that, in general, an increase in the dissociation energy results in an increase of the internal energy of the photofragments. However, in the present experiment, the low-energy region of the absorption band corresponds to the high vibrational band of NO. This coincidence further supports the above conclusion that *o*-nitrotoluene imparts a higher vibrational energy in NO than nitrobenzene and that this result is not caused by an increased excitation energy. The relative population between spin−orbit states of NO in the current work shows the same trend as that from nitromethane, in which the $^2\Pi_{1/2}$ component was preferentially populated by a factor of 2:1.[7]

B. Orientation Effect on the Yield of NO. To obtain the direction of the transition dipole, we performed polarization spectroscopy on oriented *o*-nitrotoluene parent molecules. For an effectively oriented system, the direction of the transition dipole can be obtained from the dependence of the yield of photofragments on the polarization direction of the dissociation laser. When the laser is polarized parallel to the orientation field, preferential excitation through a transition dipole parallel to the field is accomplished. Conversely, when the laser is polarized perpendicular to the orientation field, only surfaces accessible through a transition dipole perpendicular to the electric field are involved. We will quantify polarization effects of the dissociation laser by defining a polarization ratio, ρ, as the ratio of the yield of NO fragments when the dissociation laser is polarized perpendicular/parallel to the orientation field.

A few rotational transitions from the $v'' = 0$, 1, and 2 vibrational bands were used to measure effects of the polarization direction of the dissociation laser. Table 2 lists experimentally determined values of ρ in an orientation field of 50 kV/cm. Rotational transitions listed with a slash between them were too close in wavelength to be resolved with the current laser system. High rotational levels dominate these transitions, and this choice was based on several considerations, in addition to line intensity and line shape. First, high J levels are free of contamination from dissociation products of clusters. The cooling effect of a cluster on the final state rotational distribution has been documented from dissociation of *tert*-butyl nitrite.[50] The high J levels in this study should therefore not be substantially populated from dissociation of nitrotoluene clusters. Although great care has been taken to avoid formation of

TABLE 2: Polarization Ratios of the NO Fragment from Photodissociation of *o*-Nitrotoluene between 220 and 250 nm[a]

	$v'' = 0$	$v'' = 1$	$v'' = 2$
$Q_2(54.5)/P_1(61.5)$	1.47 ± 0.06		
$P_2(37.5)/R_{21}(16.5)$	1.47 ± 0.05		
$P_2(47.5)/Q_1(39.5)$	1.45 ± 0.06		
$P_1(18.5)/R_2(24.5)/R_2(12.5)/R_{21}(0.5)$		1.45 ± 0.05	
$P_1(17.5)/Q_1(8.5)/R_1(2.5)/R_{21}(0.5)$			1.46 ± 0.06

[a] The ratio represents the yield of NO when the dissociation laser was polarized perpendicular/parallel to the orientation field of 50 kV/cm.

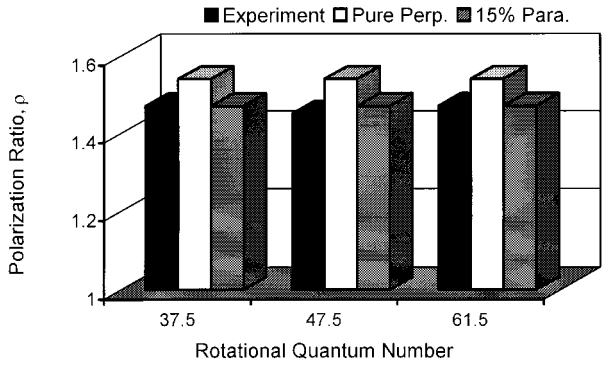

Figure 5. Polarization ratios for a few rotational transitions of the P_2 branch of the $v'' = 0$ band. Calculations of the polarization ratio for a pure perpendicular transition and a transition with 15% parallel character are also shown.

clusters, it is still prudent to avoid contamination at all stages of the measurement. Second, this choice ensures that there are no complications due to orientation of the NO fragments by the electric field. As discussed in our previous work on *tert*-butyl nitrite,[45] Stark effects on these highly rotationally excited, slightly polar (0.148 ± 0.002 D)[51] radicals are negligible. In the present experiment, the average value of ρ was 1.46, indicating a predominantly perpendicular relationship between the permanent dipole moment and the transition dipole moment. The polarization ratio was virtually independent of rotational and vibrational quantum numbers, implying that the potential energy surface(s) involved have similar topography.

Figure 5 illustrates the relationship between ρ and rotational quantum number for the $v'' = 0$ vibrational band. The expected value of ρ for a pure perpendicular transition was calculated according to the procedure outlined in a previous publication,[43] and the result is also given in Figure 5. The calculation assumed a permanent dipole moment of 3.6 D and a rotational temperature of 2.5 K. Rotational constants were obtained from an ab initio calculation at the 6-31G** level. The same calculation for nitrobenzene gave rotational constants in very good agreement with those reported by Ribeaud et al.;[52] however, the calculated permanent dipole of nitrobenzene was 30% larger than experimentally determined values. For *o*-nitrotoluene, experimental measurements of the permanent dipole varied between 3 and 4 D.[53] If a scaling factor of 70% was applied to our ab initio calculation for *o*-nitrotoluene, the resulting value was 3.6 D. This value was in very good agreement with the experiment by Rahman et al.[54] and was thus used in subsequent calculations. The direction of the permanent dipole was assumed to be along the *A* inertial axis. Calculations with the dipole along different axes yielded nearly identical results for ρ, with an error of less than 1%. The effect of the direction of the permanent dipole has been discussed in a previous publication.[55]

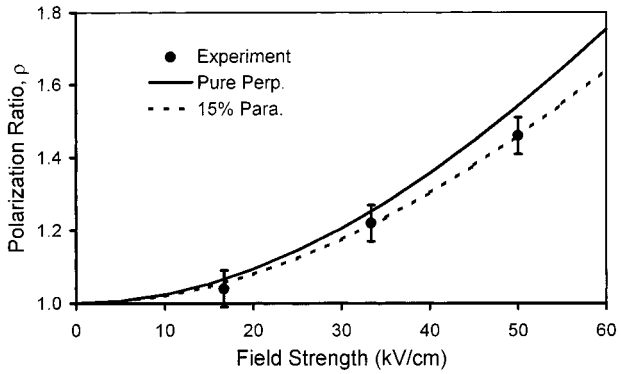

Figure 6. Dependence of the polarization ratio of the $P_2(37.5)/R_{21}(16.5)$ transition on the strength of the orientation field. As the field strength increased, more molecules became oriented, and the preference for the perpendicular polarization direction of the dissociation laser increased. For comparison, the trends for a pure perpendicular transition and a transition with 15% parallel character are given.

The experimental polarization ratios in Figure 5 are slightly less than those expected of a pure perpendicular transition. Since contribution from a parallel transition will decrease the polarization ratio due to preference of the parallel polarization direction of the photolysis laser, a second potential energy surface accessible through a parallel transition is likely present. When 15% parallel character is factored into the calculation, the agreement between theory and experiment is very good. As mentioned in the Experimental Section, the rotational temperature of 2.5 K used in our calculations is a cautious estimate. The rotationally resolved REMPI spectra of pyrimidine obtained under identical experimental conditions did not fit the simulation spectra ideally, so the resulting rotational temperature is between 2.2 and 2.6 K. This corresponds to a range between 6 and 20% for the parallel component.

The dependence of ρ on the strength of the orientation field is given in Figure 6. The experimental points represent the polarization ratio of the $P_2(37.5)/R_{21}(16.5)$ transition of the $v'' = 0$ band. Since all data were normalized with respect to field-free conditions, ρ has a value of unity at a field strength of 0 kV/cm, and the measurement contains no information on rotational alignment. As the field strength was increased, more molecules became oriented, and the preference for a perpendicularly polarized dissociation beam increased. The solid line in the figure shows the calculated polarization ratio for a pure perpendicular transition, while the dashed line factors in 15% contribution from a parallel transition. The experimental data agrees well with the latter calculation. Again, these results are supportive of the presence of a second potential energy surface in the dissociation process.

Our results are consistent with previous observations of nitromethane, nitroethane, 1-nitropropane, and nitrobenzene.[1−23,46] For nitromethane, dissociation is instantaneous, so photofragment translational spectroscopy has been used to determine vectorial information. Butler et al.[1] found that the transition dipole of nitromethane at 193 nm was perpendicular to the C_{2v} symmetry axis of the NO_2 group. However, the anisotropy parameter (β) deviated from a pure perpendicular transition. It was suggested that a change in symmetry of the NO_2 group resulted in configuration interaction between $^1B_2$ and $^1A_1$ states, tilting the direction of the effective transition dipole. Kwok et al.[8] measured gas phase absorption spectra and resonance Raman intensities of nitroethane and 1-nitropropane and reported a predissociative mechanism. Although the direction of the transition dipole moment was not specifically pursued in their experiment, the results indicated a mixing of states. Using the

same technique as that of the current work, our group measured the direction of the transition dipole of nitrobenzene between 230 and 250 nm.[46] The relationship between the permanent dipole and the transition dipole was also found to be predominantly perpendicular in nature, with 20% contribution from a parallel transition. This similarity implies a localized nature of the electronic orbitals in these nitro compounds. Confirmation of this conclusion through investigations of the other two nitrotoluene isomers is in progress.

4. Conclusions

The dissociation dynamics of *o*-nitrotoluene was explored through measurements of the NO fragment. Although qualitative, our results revealed some significant similarities and differences between *o*-nitrotoluene and nitrobenzene. Under field-free conditions, *o*-nitrotoluene yielded NO fragments in $v'' = 0$, 1, and 2 states. Upon excitation between 220 and 250 nm, the relative vibrational populations were 1:0.6:0.06. The NO fragments were formed with more vibrational energy than those from nitrobenzene as reported by Galloway et al.[18] and Daugey et al.[23] Our results were consistent with observations by Marshall et al. on *o*-nitrotoluene,[17] in which the NO fragments were vibrationally more excited than those from both nitrobenzene and nitrogen dioxide. Rotational distributions of each vibrational level were non-Boltzmann, and high rotational excitation was observed for $v'' = 0$ and 1. On the basis of the analysis of the Crim group on nitrobenzene, the energy partitioning in these nitroaromatic compounds was better described by the statistical model than the impulsive model.[18] Preferences for spin−orbit and Λ-doublet states were observed in the present experiment. The F_1/F_2 ratio was 1.4 while the A'/A'' ratio was 1.7. The latter ratio indicated that the unpaired π lobe of the NO fragment was parallel to the plane of rotation. The preference for the F_1 component ($^2\Pi_{1/2}$ spin−orbit state) showed the same trend as the NO fragment from dissociation of nitromethane at 193 nm, as reported by Moss et al.[7]

The direction of the transition dipole moment was determined from polarization spectroscopy of oriented parent molecules. In a strong, uniform electric field, the yield of NO fragments was enhanced by 46% when the polarization direction of the photolysis laser was perpendicular to the orientation field. A predominantly perpendicular relationship between the permanent dipole and the transition dipole was therefore established. Calculations assuming 15% contribution from a second potential energy surface, accessible through a parallel transition, agreed well with the experimental data. However, this quantitative result should be regarded as a cautious estimate for the parallel component in the overall oscillator strength due to the uncertainty in the rotational temperature. These results were very similar to our previous observations of nitrobenzene.[46] Considering the similarities in the UV absorption spectra of these two compounds and the probable localization of electronic orbitals on the NO_2 moiety, this conclusion was not surprising.

This work has reiterated the advantages of using a uniform electric field to determine directions of transition dipoles. This procedure is only related to the excitation probability of an oriented system under two different polarization directions of the excitation laser. It is therefore independent of the dissociation mechanism. At a fixed excitation energy, the yield of NO should be directly proportional to the excitation probability, regardless of its origin. Furthermore, this new approach is different from Doppler or other photofragment translational spectroscopic techniques. It suffers no kinematic constraints, and it can be used for large, complex systems where slow, nonenergetic fragments are produced.

Acknowledgment. We would like to thank Dr. Jorge Luque for the use of the LIFBASE spectral simulation program. This work was supported by the National Science Foundation, Division of Chemistry through the Faculty Early Career Development program. W.K. is an Alfred P. Sloan research fellow.

References and Notes

(1) Butler, L. J.; Drajnovich, D.; Lee, Y. T.; Ondrey, G.; Bersohn, R. *J. Chem. Phys.* **1983**, *79*, 1708.
(2) Rockney, B. H.; Grant, E. R. *J. Chem. Phys.* **1983**, *79*, 708.
(3) Wodtke, A. M.; Hintsa, E. J.; Lee, Y. T. *J. Phys. Chem.* **1986**, *90*, 3549.
(4) Zabarnick, S.; Fleming, J. W.; Baronavski, A. P. *J. Chem. Phys.* **1986**, *85*, 3395.
(5) Greenblatt, G. D.; Zuckermann, H.; Haas, Y. *Chem. Phys. Lett.* **1987**, *134*, 593.
(6) Lao, K. Q.; Jensen, E.; Kash, P. W.; Butler, L. J. *J. Chem. Phys.* **1990**, *93*, 3958.
(7) Moss, D. B.; Trentelman, K. A.; Houston, P. L. *J. Chem. Phys.* **1991**, *96*, 237.
(8) Kwok, W. M.; Hung, M. S.; Phillips, D. L. *Mol. Phys.* **1996**, *88*, 517.
(9) Zuccarello, F.; Millefiori, S.; Buemi, G. *Spectrochim. Acta* **1979**, *35A*, 223.
(10) Bigelow, R. W.; Freund, H.; Dick, B. *Theor. Chim. Acta* **1983**, *63*, 177.
(11) Malar, E. J. P.; Jug, K. *J. Phys. Chem.* **1984**, *88*, 3508.
(12) Gonzalez, A. C.; Larson, C. W.; McMillen, D. F.; Golden, D. M. *J. Phys. Chem.* **1985**, *89*, 4809.
(13) Tsang, W.; Robaugh, D.; Mallard, W. G. *J. Phys. Chem.* **1986**, *90*, 5968.
(14) McLuckey, S. A.; Glish, G. L. *Org. Mass Spectrom.* **1987**, *22*, 224.
(15) Gonzalez-Lafont, A.; Lluch, J. M.; Bertran, J.; Marquet, J. *Spectrochim. Acta* **1988**, *44A*, 1427.
(16) Shao, J.; Baer, T. *Int. J. Mass Spectrom. Ion Processes* **1988**, *86*, 357.
(17) Marshall, A.; Clark, A.; Ledingham, K. W. D.; Sander, J.; Singhal, R. P. *Int. J. Mass Spectrom. Ion Processes* **1993**, *125*, R21.
(18) Galloway, D. B.; Glenewinkel-Meyer, T.; Bartz, J. A.; Huey, L. G.; Crim, F. F. *J. Chem. Phys.* **1994**, *100*, 1946.
(19) Glenewinkel-Meyer, T.; Crim, F. F. *J. Mol. Struct: THEOCHEM* **1995**, *337*, 209.
(20) Kosmidis, C.; Ledingham, K. W. D.; Kilic, H. S.; McCanny, T.; Singhal, R. P.; Langley, A. J.; Shaikh, W. *J. Phys. Chem. A* **1997**, *101*, 2264.
(21) Takezaki, M.; Hirota, N.; Terazima, M.; Sato, H.; Nakajima, T.; Kato, S. *J. Phys. Chem. A* **1997**, *101*, 5190.
(22) Shishkov, I. F.; Vilkov, L. V.; Kovacs, A.; Hargittai, I. *J. Mol. Struct.* **1998**, *445*, 259.
(23) Daugey, N.; Shu, J.; Bar, I.; Rosenwaks, S. *Appl. Spectrosc.* **1999**, *53*, 57.
(24) Parker, D. H.; Bernstein, R. B. *Annu. Rev. Phys. Chem.* **1989**, *40*, 561.
(25) Janssen, M. H. M.; Parker, D. H.; Stolte, S. J. *J. Phys. Chem.* **1991**, *95*, 8142.
(26) Bulthuis, J.; van Leuken, J.; Stolte, S. J. *J. Chem. Soc., Faraday Trans.* **1995**, *91*, 205.
(27) Saleh, H. J.; McCaffery, A. J. *J. Chem. Soc., Faraday Trans.* **1993**, *89*, 3217.
(28) Weida, M. J.; Nesbitt, D. J. *J. Chem. Phys.* **1994**, *100*, 6372.
(29) Zare, R. N. *Ber. Bunsen-Ges. Phys. Chem.* **1982**, *86*, 422.
(30) Friedrich, B.; Herschbach, D. J. *J. Phys. Chem. A* **1995**, *99*, 15686.
(31) Loesch, H. J.; Remscheid, A. *J. Phys. Chem.* **1991**, *95*, 8194.
(32) Block, P. A.; Bohac, E. J.; Miller, R. E. *Phys. Rev. Lett.* **1992**, *68*, 1303.
(33) Friedrich, B.; Herschbach, D. R.; Rost, J.-M.; Rubahn, H-G.; Renger, M.; Verbeek, M. *J. Chem. Soc., Faraday Trans.* **1993**, *89*, 1539.
(34) Oudejans, L.; Miller, R. E. *J. Phys. Chem.* **1995**, *99*, 13670.
(35) Van Leuken, J. J.; Bulthuis, J.; Stolte, S.; Loesch, H. J. *J. Phys. Chem.* **1996**, *100*, 16066.
(36) Oudejans, L.; Miller, R. E. *J. Phys. Chem. A* **1997**, *101*, 7582.
(37) Loesch, H. J.; Remscheid, A. *J. Chem. Phys.* **1990**, *93*, 4779.
(38) Stolte, S. *Nature* **1991**, *353*, 391.
(39) Friedrich, B.; Herschbach, D. R. *Nature* **1991**, *353*, 412.
(40) Franks, K. J.; Li, H.; Hanson, R. J.; Kong, W. *J. Phys. Chem. A* **1998**, *102*, 7881.
(41) Li, H.; Franks, K. J.; Hanson, R. J.; Kong, W. *J. Phys. Chem. A* **1998**, *102*, 8084.
(42) Franks, K. J.; Li, H.; Kong, W. *J. Chem. Phys.* **1999**, *110*, 11779.
(43) Franks, K. J.; Li, H.; Kong, W. *J. Chem. Phys.* **1999**, *111*, 1884.
(44) Franks, K. J.; Li, H.; Kuy, S.; Kong, W. *Chem. Phys. Lett.* **1999**, *302*, 151.

(45) Castle, K. J.; Kong, W. *J. Chem. Phys.* **2000**, *112*, 10156.
(46) Castle, K. J.; Abbott, J.; Peng, X.; Kong, W. *J. Chem. Phys.* **2000**, *113*, 1415.
(47) Herzberg, G. *Molecular Spectra and Molecular Structure, I. Spectra of Diatomic Molecules*; Van Nostrand Reinhold: New York, 1950.
(48) Luque, J.; Crosley, D. R. *LIFBASE: Database and Spectral Simulation Program (Version 1.5)*; SRI International Report MP 99-009; 1999.
(49) Engleman, R.; Rouse, P. E.; Peek, H. M.; Baiamonte, V. D. *Beta and Gamma Band Systems of Nitric oxide*; Los Alamos Scientific Laboratory of the University of California: Los Alamos, NM, 1970.
(50) Kades, E.; Rösslein, M.; Brühlmann, U.; Huber, J. R. *J. Phys. Chem.* **1993**, *97*, 989.
(51) Roberts, L. H.; Mathur, M. S.; Kadaba, P. K. *IEEE Trans. Instrum. Meas.* **1968**, *17*, 192.
(52) Ribeaud, M.; Bauder, A.; Gunthard, H. H. *Mol. Phys.* **1972**, *23*, 235.
(53) McClellan, A. L. *Tables of Experimental Dipole Moments, Volume 2*; Rahara Enterprises: El Cerrito, CA, 1974.
(54) Rahman, S. M. F.; Roy, A. N.; Bhattacharya, J. R. *J. Nat. Sci. Math.* **1965**, *5*, 203.
(55) Kong, W.; Bulthuis, J. *J. Phys. Chem. A* **2000**, *104*, 1055.